Biochemical and Biophysical Research Communications 432 (2013) 519–525

Contents lists available at SciVerse ScienceDirect

Biochemical and Biophysical Research Communications

journal homepage: www.elsevier.com/locate/ybbrc

Ablation of *Rnf213* retards progression of diabetes in the Akita mouse

Hatasu Kobayashi [a,1], Satoru Yamazaki [b,1], Seiji Takashima [c], Wanyang Liu [a], Hiroko Okuda [a], Junxia Yan [a], Yukiko Fujii [a], Toshiaki Hitomi [a], Kouji H Harada [a], Toshiyuki Habu [d], Akio Koizumi [a,*]

[a] Department of Health and Environmental Sciences, Graduate School of Medicine, Kyoto University, Kyoto, Japan
[b] Department of Cell Biology, National Cerebral and Cardiovascular Center, Suita, Osaka, Japan
[c] Department of Molecular Cardiology, Osaka University, Suita, Osaka, Japan
[d] Radiation Biology Center, Kyoto University, Kyoto, Japan

ARTICLE INFO

Article history:
Received 23 January 2013
Available online 11 February 2013

Keywords:
Rnf213
Moyamoya disease
Diabetes
Knockout mouse
Akita mouse

ABSTRACT

Moyamoya disease (MMD) and moyamoya syndrome are vasculopathies characterized by progressive stenosis in the circle of Willis and its branches. The *RNF213* gene, which encodes a novel class of proteins, characterized by both E3 ligase and AAA + ATPase activities, has been identified as the susceptibility gene for MMD. However, its physiological functions remain unknown. MMD and moyamoya syndrome are often accompanied by diabetes mellitus. In this study, we generated *Rnf213* knockout (KO) C57BL/6 mice (*Rnf213*$^{-/-}$; *Ins2*$^{+/+}$), which were mated with Akita (C57BL/6 *Rnf213*$^{+/+}$; *Ins2*$^{+/C96Y}$) mice, a strain that develops diabetes spontaneously by 5 weeks of age, to obtain mice lacking *Rnf213* and carrying the Akita mutation (KO/Akita, *Rnf213*$^{-/-}$; *Ins2*$^{+/C96Y}$). Body weight and blood glucose concentration were measured from 6 to 20 weeks. Glucose tolerance, insulin resistance, plasma insulin and leptin concentrations, food consumption, pancreatic insulin content and histopathology were evaluated at 18 weeks of age. We found that glucose tolerance, as indicated by AUC, was 20% lower ($p < 0.05$) and insulin contents in pancreas were 150% higher ($p < 0.05$), in KO/Akita than in Akita mice. The number of CHOP positive β-cells assayed by histopathological examination was 30% lower and food consumption was 34% lower in KO/Akita than in Akita mice ($p < 0.05$ each). These findings indicated that the disruption of *Rnf213* improved glucose tolerance by protecting islet β cells.

1. Introduction

Moyamoya disease (MMD) and moyamoya syndrome are vasculopathies characterized by occlusion at the internal carotid arteries in the circle of Willis and the compensatory formation of an abnormal vascular network, resembling "puffs of smoke", that are called moyamoya vessels [1]. Patients with moyamoya syndrome have a predisposing disease [2], including Down's syndrome [3], neurofibromatosis 1 [4], or microcephalic osteodysplastic primordial dwarfism type Majewski II (MOPDII) [5], whereas patients with MMD have no such predisposing conditions.

Conditions predisposing to moyamoya syndrome are frequently accompanied by diabetes [2,5–7]. Moreover, the prevalence of type 1 diabetes mellitus was shown to be much higher in patients with MMD than in the general population [8], suggesting a pathological link between MMD and diabetes. We recently demonstrated that *RNF213* was the susceptibility gene for MMD, and that the p.R4810K polymorphism (ss179362673: G>A) is a founder variant commonly found in East Asian patients [9]. Although knockdown of *RNF213* in zebrafish caused abnormal vascular development [9], the physiological function of *RNF213* remains largely unknown.

RNF213 encodes a unique, 591-kDa protein with both a ring finger domain and Walker motifs, and *RNF213* mRNA is expressed in various tissues [9]. The E3 ligase activity of the ring finger domain was confirmed by self-ubiquitination, and ATPase in the Walker motifs was confirmed biochemically [9]. Ring-base E3 ligases have been linked to the control of many cellular processes, including proteasome-dependent proteolysis, DNA repair, signal transduction, apoptosis, immunological processes and transcription [10]. *RNF213* is also an AAA + ATPase because it has Walker A and Walker B motifs. AAA + ATPases usually exist and function as oligomers; their cellular functions include vesicular transport, quality control, cargo trafficking and microtubule homeostasis [11].

In this study, we tested whether ablation of *Rnf213* can modify diabetes mellitus in Akita mice (C57BL/6 *Rnf213*$^{+/+}$; *Ins2*$^{+/C96Y}$), a model for type 1 diabetes [12], in which β-cell destruction results from endoplasmic reticulum (ER) stress. We found that ablation of *Rnf213* unexpectedly alleviates diabetes by preserving β-cell function through moderating the vicious cycle of hyperphagia and hypoinsulinemia.

* Corresponding author. Address: Department of Health and Environmental Sciences, Graduate School of Medicine, Kyoto University, Konoe-cho, Yoshida, Sakyo-ku, Kyoto 606-8501, Japan. Fax: +81 75 753 4458.
E-mail address: koizumi.akio.5v@kyoto-u.ac.jp (A. Koizumi).
[1] These authors contributed equally to this work.

0006-291X/$ - see front matter © 2013 Elsevier Inc. All rights reserved.
http://dx.doi.org/10.1016/j.bbrc.2013.02.015

2. Materials and methods

2.1. Generation of Rnf213 knockout mice

An *Rnf213*-targeting construct was produced using a Multisite Gateway Three-Fragment Vector Construction Kit (Invitrogen). Briefly, a loxP site was cloned into the 5′ site of exon 20, and a fragment containing a loxP site and a neomycin-resistance gene (Neo) was cloned into the 3′ site of exon 20 (Fig. 1A, Supplemental material). The construct was linearized and electroporated into RENKA C57BL/6 ES cells and selected with G418. Integration of the targeting vector into the mouse genome by homologous recombination was verified in targeted ES clones by Southern blotting (data not shown). Correctly targeted clones were injected into C57BL/6 blastocysts to generate chimeric mice with the targeted allele incorporated into the germ lines. The resulting chimeric male mice were mated with female C57BL/6 mice, and germ line transmission of the targeted allele was examined in the offspring. Offspring carrying the target allele were bred with Cre-transgenic C57BL/6 mice to generate mice heterozygous for the *Rnf213* deficiency ($Rnf213^{-/+}$). Heterozygous male and female mice were bred to produce homozygous offspring (KO, $Rnf213^{-/-}$).

2.2. Experimental animals

Akita ($Ins2^{+/C96Y}$) mice on a C57BL/6 background and C57BL/6 (WT) mice were purchased from Japan SLC. To generate mice lacking *Rnf213* and carrying the Akita mutation (KO/Akita, $Rnf213^{-/-}$; $Ins2^{+/C96Y}$), male double-heterozygous ($Rnf213^{+/-}$; $Ins2^{+/C96Y}$) mice were generated and mated with female *Rnf213* KO mice. Experiments were performed on four groups of male mice: (1) KO/Akita ($Rnf213^{-/-}$; $Ins2^{+/C96Y}$), (2) Akita ($Rnf213^{+/+}$; $Ins2^{+/C96Y}$), (3) KO ($Rnf213^{-/-}$; $Ins2^{+/+}$), and (4) WT ($Rnf213^{+/+}$; $Ins2^{+/+}$). Progeny of (1–3), aged 4 weeks, were selected by PCR genotyping for *Rnf213* (Supplemental material) and the *Ins2* locus, as described [13]. Mice were allowed free access to a standard diet (CLEA, Rodent Diet CE-7, 3.4 kcal/g) and tap water. The care of the animals and all experimental procedures were in accordance with the Animal Welfare Guidelines of Kyoto University.

2.3. Culture of Akita and min-6 cell lines and real-time PCR (RT-PCR)

To test *Rnf213* expression in β cells, we used Akita cells and the min-6 cell line [14,15]. Quantitative RT-PCR for *Rnf213* was performed using the specific primers, Rnf213cex29–31F (5′-TAA GGA TGT CCG CTC CTG GTT-3′) and Rnf213cex29–31R (5′-TTG ATG GCA GTA TAC TTG GCA-3′).

2.4. Western blotting

Protein samples from mice pancreas or cultured cells were subjected to immunoblotting using the rabbit polyclonal anti-RNF213 antibody and anti-GAPDH antibody (Santa Cruz Biotechnology). The rabbit polyclonal antibody was produced by inoculation of rabbits with cloned human full-length RNF213 as an antigen. The polyclonal IgG was purified from rabbit serum.

2.5. Measurement of glucose, insulin, proinsulin and leptin

Blood glucose was measured by Glutest Neo Super (Sanwa). All values above 600 mg/dl were treated as 600 mg/dl. Glucose tolerance testing (GTT) was performed by fasting 18-week-old mice for 16 h, followed by an intraperitoneal injection of 1.5 g/kg glucose. Insulin tolerance testing (ITT) was performed by fasting 18-week-old mice for 6 h, followed by an intraperitoneal injection of 1.5 U/kg insulin (Eli Lilly and Company). To measure leptin concentrations, blood was collected from the tail veins of 18-week-old mice after a 16 h fast. Plasma concentrations of insulin, leptin and proinsulin were measured by ELISA (Shibayagi).

2.6. Measurement of pancreatic insulin and proinsulin contents

Mice were sacrificed at 18 weeks of age in the morning after a 6 h fast. Each pancreas was homogenized in acid ethanol (75% ethanol, 1.5% HCl) and extracted at 4 °C overnight. The extracts were centrifuged, and the insulin and proinsulin concentrations of the supernatants were measured.

2.7. Pathological investigations

Mice were sacrificed under sevoflurane at 18 weeks of age after a 6 h fast. Each pancreas was fixed in 10% formaldehyde, embedded in paraffin, and sectioned. The sections were immunostained with guinea pig anti-insulin antibody (Dako) or rabbit anti-C/EBP homologous protein (CHOP)/GADD153 antibody (Santa Cruz Biotechnology). To estimate β-cell mass, consecutive paraffin sections 75 μm apart and spanning the entire pancreas (5–8 sections per pancreas) were prepared, and islet areas and relative abundance of insulin- and CHOP-positive cells were quantified on more than 20 islets per pancreas in three or four mice per genotype using Image-J software (National Institutes of Health). For electron microscopy, pancreases were fixed in 2% glutaraldehyde and post-fixed in 1% osmium tetroxide.

2.8. Statistical analysis

Results are presented as the mean ± standard deviation (SD) or standard error (SE). Differences were analyzed by *t*-test or ANOVA followed by Tukey's honestly significant difference test using STATISTICA software (StatSoft). $p < 0.05$ was considered statistically significant.

3. Results

3.1. General characterization of Rnf213 KO mice

To determine the physiological function of *Rnf213*, we generated mice with targeted deletion of *Rnf213* exon 20. This targeting strategy, in which a frame shift mutation was introduced into this exon, resulted in the disruption of the Walker motifs and the ring finger domain (Fig. 1A). Complete removal of *Rnf213* exon 20 from genomic DNA (Fig. 1B) and the absence of Rnf213 protein expression (Fig. 1C), were confirmed in KO mice. KO mice were born in the predicted Mendelian ratio and did not show any apparent health problems, including a cerebrovascular phenotype similar to MMD, even at around 80 weeks of age. Both males and females were fertile and produced normal-sized litters (mean, 6–8 pups). The body weight of KO mice was about 13% less than that of WT mice after 25 weeks of age ($p < 0.05$), and GTT results in KO and WT mice did not differ at 50 weeks of age (Supplemental Fig. 1).

3.2. Expression of Rnf213 in Akita and min-6 cells

Rnf213 protein was expressed in the pancreas (Fig. 1C). To assess the expression of *Rnf213* in β cells, we investigated the expression of *Rnf213* mRNA and protein in Akita and min-6 cell lines by quantitative RT-PCR and western blotting, respectively. We found that *Rnf213* mRNA and protein were expressed in these cells, with no differences between Akita and min-6 cell lines (Fig. 1D and E).

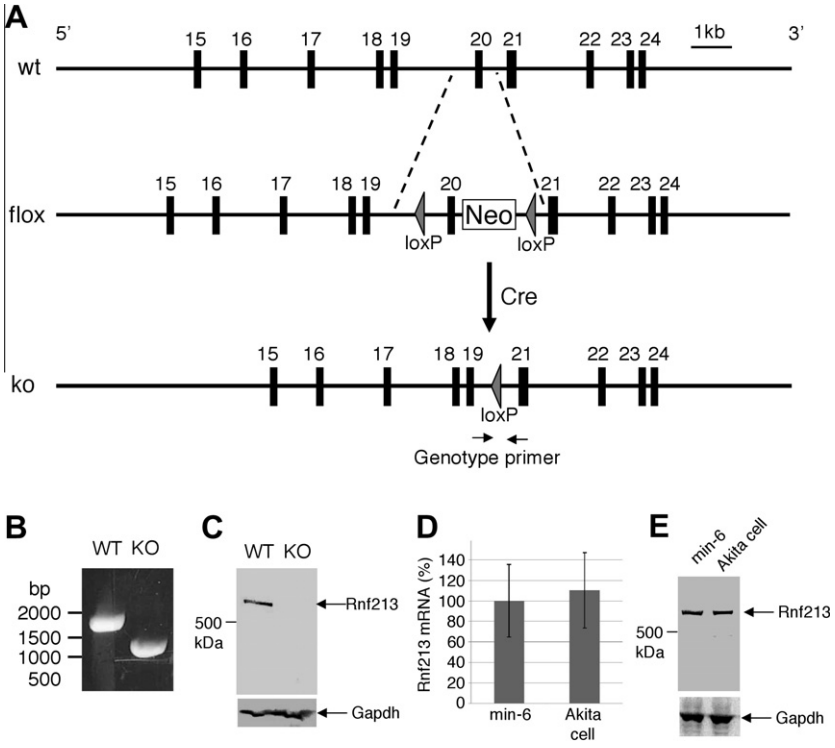

Fig. 1. Generation of *Rnf213* KO mice. (A) Structure of the endogenous mouse *Rnf213* gene, the targeted allele, and the disrupted allele. (B) PCR genotyping of WT and KO mice. (C) *Rnf213* immunoblotting of pancreas extracts from WT and KO mice. (D) Quantitative RT PCR for *Rnf213* in Akita and min-6 cells. Data are shown as mean ± SD. (E) *Rnf213* immunoblotting of extracts from Akita and min-6 cells. Membranes were immunoblotted with antibody to GAPDH as a loading control.

3.3. Body weight over time

The mean body weight of KO/Akita mice was lower than that of Akita mice between 6 and 9 weeks of age, although they did not differ after 10 weeks of age (Fig. 2A). The mean body weights of both KO/Akita and Akita mice were significantly lower than those of KO and WT mice. Between 6 and 20 weeks of age, there were no differences in body weight between KO and WT mice.

3.4. Blood glucose level and glucose tolerance

From 6 to 20 weeks of age, blood glucose concentrations after a 16 h fast were consistently and significantly lower in KO/Akita than in Akita mice (Fig. 2B). Moreover, blood glucose levels after a 6 h fast were significantly lower in 18 week old KO/Akita (348 ± 153 mg/dL) than in Akita (572 ± 42 mg/dL) mice, although both were significantly higher than in KO (140 ± 32 mg/dL) and WT (147 ± 22 mg/dL) mice (Fig. 2C). GTT at 18 weeks showed that glucose tolerance in KO/Akita (Area under the curve [AUC] 49298 ± 8864 mg min/dL) mice was impaired relative to KO (AUC 22179 ± 1516 mg min/dL) and WT (AUC 18284 ± 1170 mg min/dL) mice, but was better than in Akita mice (AUC 62346 ± 9105 mg min/dL) (Fig. 2D and E). These results indicated that deletion of *Rnf213* led to improvements in glucose tolerance in Akita mice. We also investigated the insulin sensitivity of KO/Akita mice. ITT at 18 weeks of age revealed no difference in insulin sensitivity among the KO/Akita, Akita, KO and WT strains (Fig. 2F).

3.5. Plasma insulin and proinsulin concentrations

Plasma insulin concentrations were significantly higher in 18 weeks old KO/Akita (1300 ± 270 pg/mL) than in Akita mice (54 ± 14 pg/mL) after a 6 h fast, but were similar in KO/Akita, KO (1466 ± 323 pg/mL) and WT (783 ± 93 pg/mL) mice (Fig 3A). Plasma insulin concentrations after fasting for 6 h and 16 h showed a significant and positive correlation with blood glucose concentrations in KO/Akita ($R = 0.50$, $p = 0.0009$), but not in Akita ($R = 0.26$, $p = 0.275$), mice (Fig. 3B), indicating that insulin secretion was responsive to increased blood glucose in KO/Akita, but not in Akita, mice. The plasma ratios of proinsulin/insulin concentrations did not differ significantly among KO/Akita, KO and WT mice (Supplemental Fig. 2A). Proinsulin was not detected in the plasma of Akita mice.

3.6. Food intake and plasma leptin concentration

Male Akita mice develop more profound diabetes than female Akita mice. Castration of male Akita mice alleviated such sex differences by reducing hyperphagia [16]. We have shown that castration normalized hyperphagia by acting on plasma leptin and normalizing anorexigenic proopiomelanocortin (POMC) [16]. To examine the regulation of feeding, we measured food consumption and plasma leptin concentration. Food consumption by KO/Akita mice (3.92 ± 0.78 g/day) was similar to that by KO (3.25 ± 0.33 g/day) and WT (3.06 ± 0.23 g/day) mice, but was 34% lower than by Akita mice (5.96 ± 0.68 g/day) (Fig. 3C). Plasma leptin concentrations were similar in KO/Akita (353 ± 226 pg/mL) and Akita (348 ± 43 pg/mL) mice, but lower than in KO (741 ± 156 pg/mL) and WT (744 ± 145 pg/mL) mice (Fig. 3D), suggesting that decreased food consumption in KO/Akita mice was likely attributable to elevated insulin concentration, which stimulates overlapping insulin-leptin signal pathways in the central nervous system to suppress appetite [17].

3.7. Pancreatic insulin and proinsulin concentration

Total pancreatic insulin levels were significantly higher in KO/Akita (2689 ± 746 ng/pancreas) than in Akita (1102 ± 43 ng/pancreas) mice, although they were about one-fifth of those in KO (14,434 ± 3359 ng/pancreas) and WT (13,348 ± 2500 ng/pancreas) mice (Fig. 4A). Pancreatic proinsulin contents were also signifi-

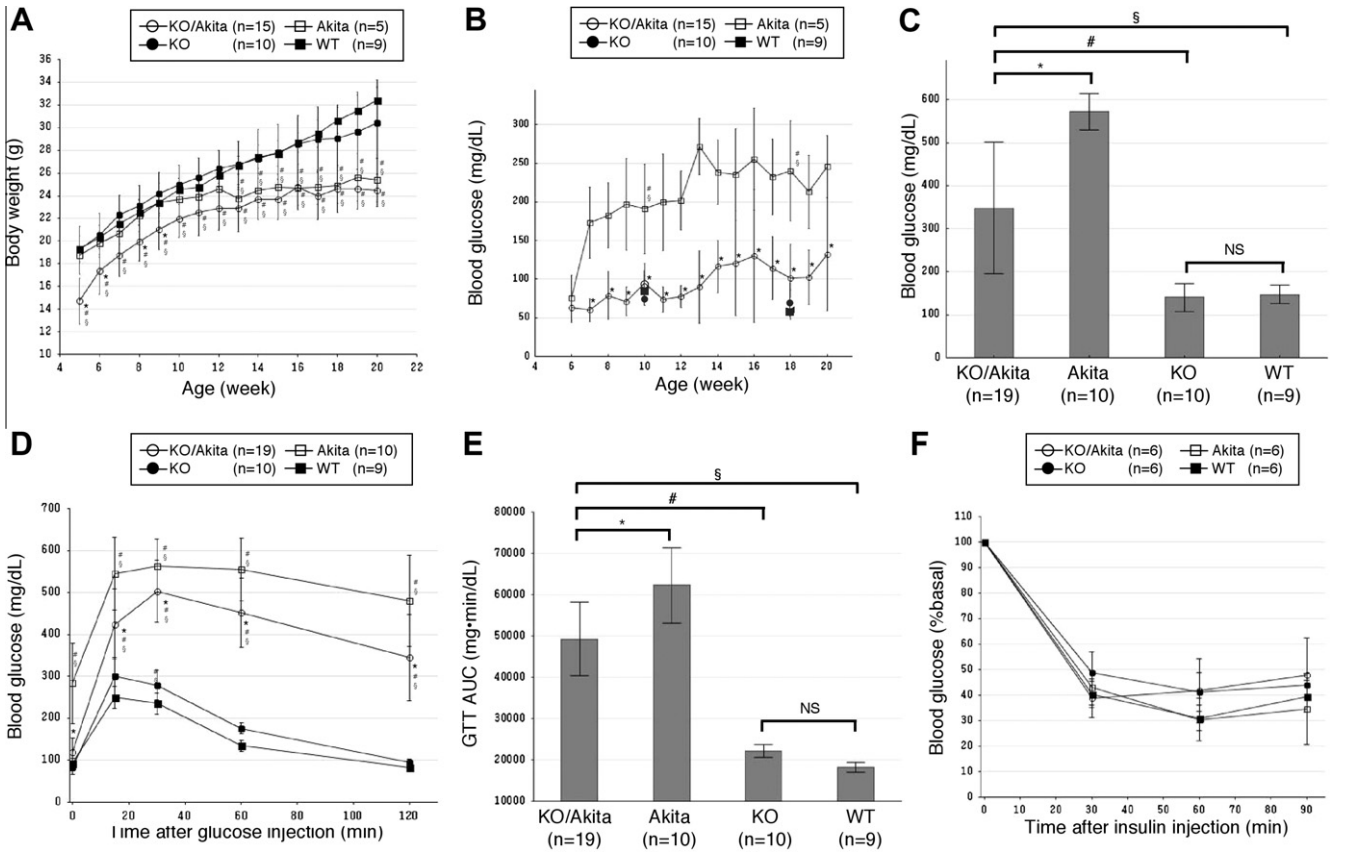

Fig. 2. Mouse growth curves, blood glucose concentrations, GTT and ITT. (A) Time course of body weight of KO/Akita, Akita, KO, and WT mice from 6 to 20 weeks of age. (B) Time course of 16 h fasting blood glucose concentrations in KO/Akita, Akita, KO and WT mice from 6 to 20 weeks of age. Glucose concentrations in KO and WT mice were measured at 10 and 18 weeks of age. (C) Six hours fasting blood glucose concentrations in 18 week old KO/Akita, Akita, KO, and WT mice. (D and E) GTT of 18 week old KO/Akita, Akita, KO, and WT mice. Blood glucose concentrations are shown at indicated times after glucose injections. Area under the curve was calculated for these mice. (F) ITT in 18 week old KO/Akita, Akita, KO, and WT mice. Blood glucose concentrations are shown at indicated times after insulin injections. Data are shown as mean ± SD. $^{*}p < 0.05$ vs Akita, $^{\#}p < 0.05$ vs KO, $^{\S}p < 0.05$ vs WT, NS, Not significant.

cantly higher in KO/Akita than in Akita mice (Supplemental Fig. 2B). Pancreas weight was similar in these 4 groups (Supplemental Fig. 3A).

3.8. Immunohistochemical assays of insulin and CHOP, and electron microscopy of islets

No morphological abnormalities were observed in the pancreas or islets of KO/Akita and KO mice. Immunohistochemical examination showed that a higher proportion of insulin-positive β cells was preserved in the islets of KO/Akita (0.141 ± 0.046 insulin positive cells/islet) than of Akita (0.088 ± 0.042 insulin positive cells/islet) mice, although both were lower than in KO (0.643 ± 0.080 insulin positive cells/islet) and WT (0.616 ± 0.076 insulin positive cells/islet) mice (Fig. 4B). Mean islet area did not differ among KO/Akita, Akita, KO and WT mice (Supplemental Fig. 3B).

CHOP is an ER stress-inducible transcription factor that promotes apoptosis [18] and that has been used as a marker of ER stress-mediated apoptosis in β cells of Akita mice [19]. To test whether ER stress occurs in the β cells of KO/Akita mice, we assayed for CHOP immunohistochemically. The percentage of CHOP-positive cells in islets was significantly lower in KO/Akita (0.102 ± 0.042 CHOP positive cells/islet) than in Akita (0.135 ± 0.037 CHOP positive cells/islet) mice, but were much lower in KO (0.002 ± 0.000 CHOP positive cells/islet) and WT (0.002 ± 0.000 (CHOP positive cells/islet) mice (Fig. 4C), indicating that ER stress is lower in the β cells of KO/Akita mice.

Electron microscopy of β cells in WT mice revealed abundant mature secretory granules in the cytoplasm, inconspicuous ER, and intact mitochondria with cristae (Fig. 4D, WT). KO mice showed no morphological abnormalities (Fig. 4D, KO). In contrast, examination of Akita mice showed a small number of secretory granules, a tubulovesicular structure comprised of markedly enlarged ER, and swelling or disruption of mitochondria (Fig 4D, Akita), indicators of insulin secretory pathway impairment and ER stress. Unlike Akita mice, KO/Akita mice showed mild ER enlargement and slight swelling of the mitochondria in β cells, although the number of secretory granules was markedly reduced (Fig. 4D, KO/Akita), suggesting less ER stress in the β cells of these mice than in Akita mice. The α cells of KO/Akita, Akita, KO and WT mice were morphologically similar (data not shown).

4. Discussion

We have shown here that targeted disruption of *Rnf213* unexpectedly improved glucose tolerance in Akita mice, although insulin sensitivity was not altered. These findings are consistent with results showing that plasma and pancreatic insulin levels were higher in KO/Akita than in Akita mice. Moreover, disruption of *Rnf213* reduced hyperphagia by elevating plasma insulin concentrations in KO/Akita, but did not alter plasma leptin concentrations in these mice. Taken together, these findings suggest that ablation of *Rnf213* may mitigate the diabetic phenotype by preserving β cell function.

Amelioration by *Rnf213* ablation contradicts a mechanistic link between MMD and diabetes [8], if variants were associated with MMD by loss-of-function or haploinsufficiency of *RNF213*. Alterna-

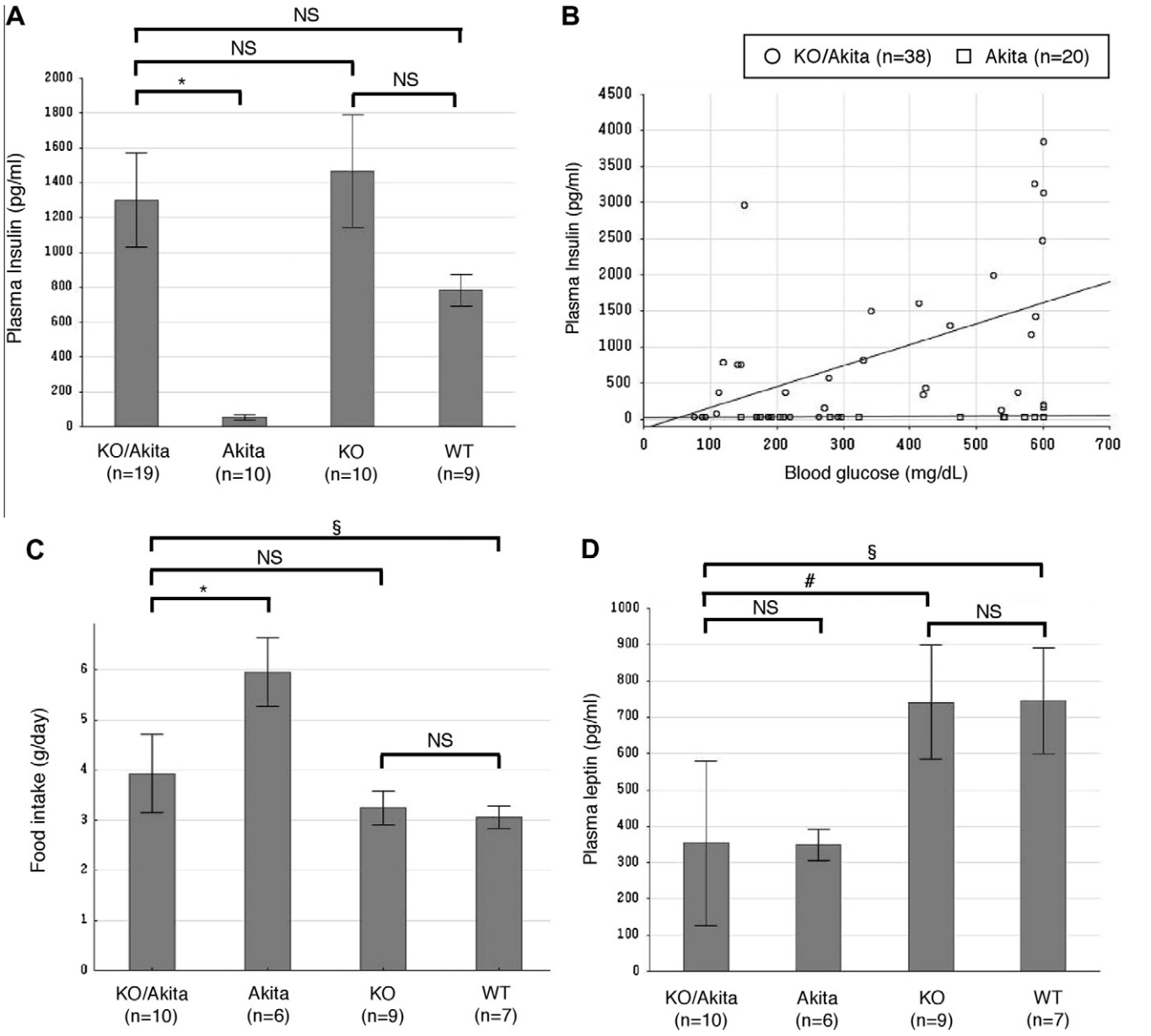

Fig. 3. Plasma insulin and leptin concentrations and food intake at 18 weeks of age. (A) Plasma insulin concentrations in KO/Akita, Akita, KO, and WT mice after a 6 h fast. Data are shown as mean ± SE. (B) Correlation between blood glucose and plasma insulin concentrations of KO/Akita and Akita mice after fasting for 6 h and 16 h (combined). (C) Food intake by KO/Akita, Akita, KO, and WT mice. (D) Plasma leptin concentrations of KO/Akita, Akita, KO, and WT mice after 16 h fasting. Data are shown as mean ± SD except for plasma insulin concentrations. $^{*}p < 0.05$ vs Akita, $^{\#}p < 0.05$ vs KO, $^{\S}p < 0.05$ vs WT, NS, not significant.

tively, pathological variants including R4810K of *RNF213* may cause MMD and diabetes by a gain-of-function or in a dominant-negative fashion. Among MMD predisposing diseases, diabetogenic mechanisms are well defined in MOPDII, a rare genetic disease characterized by severe growth retardation and early onset diabetes, as well as complication by MMD. Pericentrin, the causative gene for MOPDII, may regulate the intracellular distribution and secretion of insulin, and mutations of pericentrin may result in β-cell dysfunction [20]. The findings presented here indicate that β-cell dysfunction may have a mechanistic link with MMD.

Akita mice carrying a heterozygous C96Y mutation in the *Ins2* gene spontaneously develop hyperglycemia at an early age with reduced pancreatic β cell mass [12,13]. This C96Y mutation causes a conformational change in the insulin molecule, resulting in ER stress. ER stress, in turn, induces an unfolded protein response (UPR), indicating increased degradation of unfolded proteins by ER-associated degradation (ERAD), which is associated with E3 ligase and AAA + ATPase.

Recent studies [21,22] have demonstrated that the $Ins2^{C96Y}$ allele acts dominantly to enhance degradation of both the Akita and wild-type allele proinsulins by the ERAD pathway. We hypothesize that ablation of *Rnf213* may impair ERAD and lead to the sparing of wild-type proinsulin. Then we should explain how such preserved insulin secretion in KO/Akita mice reduced ER stress, as indicated by a reduction in the relative abundance of CHOP positive cells in these mice. Diabetes progresses more rapidly in male than female Akita mice [12]. This gender difference in susceptibility can be reversed by castration of males, thus suppressing hyperphagia [16]. Hyperphagia increases insulin demand due to elevated energy uptake, resulting in enhanced ER-stress with stimulated production of $Ins2^{C96Y}$. Such a vicious cycle may likely accelerate the progression of diabetes in male Akita mice. We found that

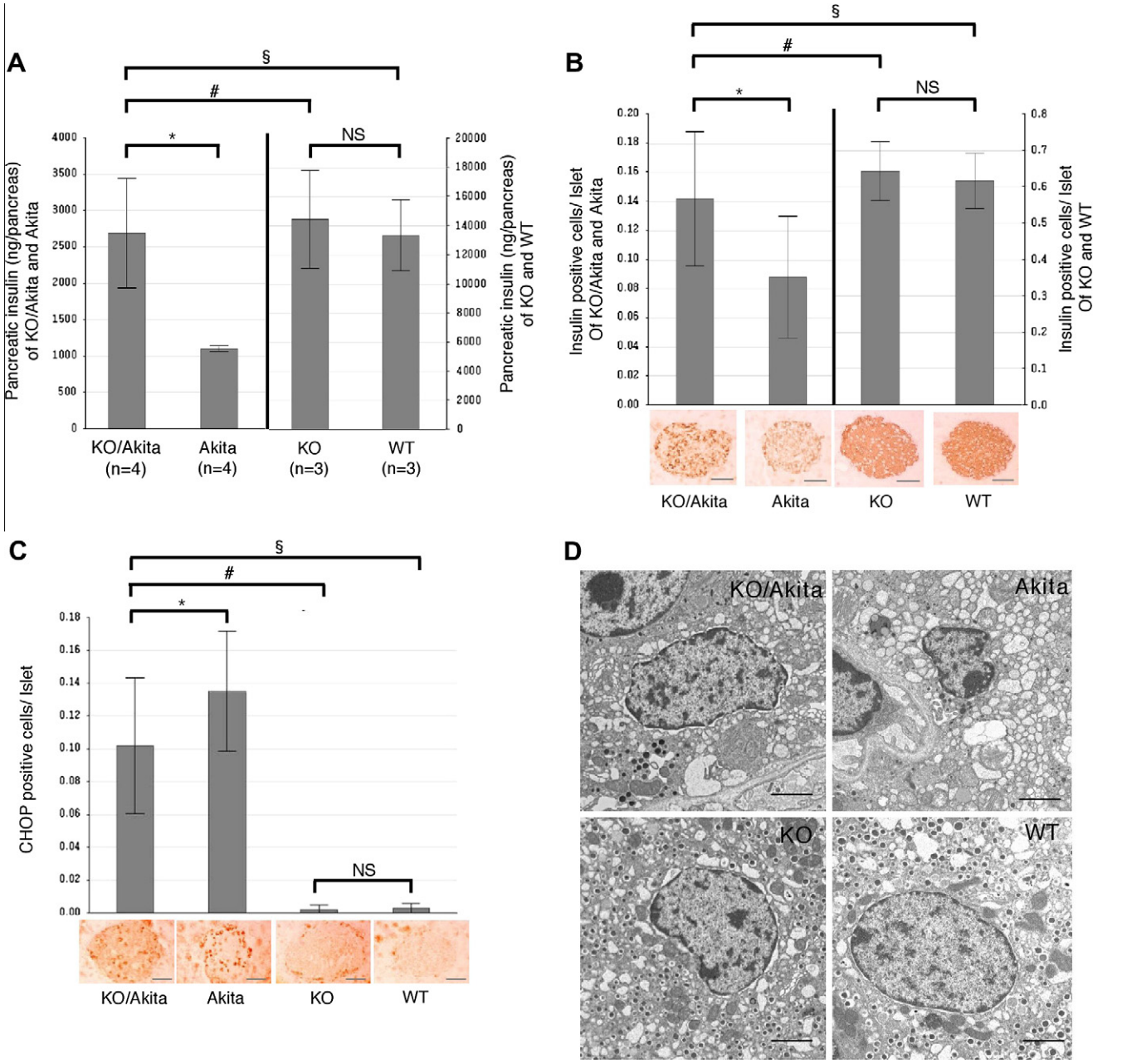

Fig. 4. Pancreatic insulin contents, insulin and CHOP immunohistochemistry, and electron microscopy of 18 week old mice. (A) Pancreatic insulin contents of KO/Akita, Akita, KO, and WT mice. (B) Representative images of islets stained with anti-insulin antibody (lower) and insulin positive cells per islet (upper) of KO/Akita ($n = 4$), Akita ($n = 4$), KO ($n = 3$), and WT ($n = 3$) mice. Quantification was performed on more than 20 islets from each mouse. Scale bar indicates 50 μm. (C) Representative images of islets stained with anti-CHOP antibody (lower) and CHOP positive cells per islet (upper) of KO/Akita ($n = 4$), Akita ($n = 4$), KO ($n = 3$), and WT ($n = 3$) mice. Quantification was performed on more than 20 islets from each mouse. Scale bar indicates 50 μm. (D) Electron micrographs of islets of KO/Akita, Akita, KO, and WT mice. Scale bar indicates 2 μm. Data are shown as mean ± SD. $^{*}p < 0.05$ vs Akita, $^{\#}p < 0.05$ vs KO, $^{\S}p < 0.05$ vs WT, NS, Not significant.

the higher serum insulin levels in KO/Akita mice were sufficient to suppress hyperphagia. Thus, *RNF213* ablation can spare wild-type insulin, thereby ameliorating this viscous cycle. Further study is warranted to test whether *RNF213* is involved in the ERAD pathway.

RNF213 is a single protein with two types of enzymatic activity, E3 ligase and AAA + ATPase [9]. AAA + ATPase is involved in various cellular processes, including vesicular transport, UPR, motor proteins and microtubule severing [11]. The association between *Rnf213* and β cell function is likely mediated by both E3 ligase and AAA + ATPase activities. The core assumption, that the normal allele of *Ins2* is also a target of degradation by ERAD, is intriguing and requires more quantitative assessment in the future. Future studies may help provide clues into a new therapeutic approach for diabetes as well as to gain insight into *RNF213* function.

Acknowledgments

This study was mainly supported by grants from the Ministry of Education, Culture, Sports, Science and Technology of Japan (Kiban Kenkyu A: 22249020) and from the Ministry of Health, Labour and Welfare of Japan (H23-Nanji-Ippan-01 and H23-Bio-Ippan-003) to AK and partially by grants from the Ministry of Education, Culture, Sports, Science and Technology of Japan (Tokubetukenkyuin

Syoreihi: 225192) to HK. We thank Ms. Emi Nakai for assistance with ES screening.

Appendix A. Supplementary data

Supplementary data associated with this article can be found, in the online version, at http://dx.doi.org/10.1016/j.bbrc.2013.02.015.

References

[1] J. Suzuki, A. Takaku, Cerebrovascular "moyamoya" disease. Disease showing abnormal net-like vessels in base of brain, Arch. Neurol. 20 (1969) 288–299.
[2] R.M. Scott, E.R. Smith, Moyamoya disease and moyamoya syndrome, N. Engl. J. Med. 360 (2009) 1226–1237.
[3] D.S. Kainth, S.A. Chaudhry, H.S. Kainth, F.K. Suri, A.I. Qureshi, Prevalence and characteristics of concurrent down syndrome in patients with moyamoya disease, Neurosurgery 72 (2013) 210–215.
[4] K. Okazaki, A. Kakita, H. Tanaka, K. Kimura, M. Minagawa, T. Morita, H. Takahashi, Widespread ischemic brain lesions caused by vasculopathy associated with neurofibromatosis type 1, Neuropathology 30 (2010) 627–633.
[5] M.B. Bober, N. Khan, J. Kaplan, K. Lewis, J.A. Feinstein, C.I. Scott Jr., G.K. Steinberg, Majewski osteodysplastic primordial dwarfism type II (MOPD II): expanding the vascular phenotype, Am. J. Med. Genet. A 152A (2010) 960–965.
[6] A.J. Anwar, J.D. Walker, B.M. Frier, Type 1 diabetes mellitus and Down's syndrome: prevalence, management and diabetic complications, Diabet. Med. 15 (1998) 160–163.
[7] M. Kamoun, N. Charfi, N. Rekik, M.F. Mnif, F. Mnif, H. Kmiha, Z. Mnif, M. Abid, Neurofibromatosis and Type 1 diabetes mellitus: an unusual association, Diabet. Med. 26 (2009) 1180–1181.
[8] R.S. Bower, G.W. Mallory, M. Nwojo, F.B. Meyer, Y.C. Kudva, Diabetes mellitus and the moyamoya syndrome, Ann. Intern. Med. 157 (2012) 387–388.
[9] W. Liu, D. Morito, S. Takashima, Y. Mineharu, H. Kobayashi, T. Hitomi, H. Hashikata, N. Matsuura, S. Yamazaki, A. Toyoda, K. Kikuta, Y. Takagi, K.H. Harada, A. Fujiyama, R. Herzig, B. Krischek, L. Zou, J.E. Kim, M. Kitakaze, S. Miyamoto, K. Nagata, N. Hashimoto, A. Koizumi, Identification of RNF213 as a susceptibility gene for moyamoya disease and its possible role in vascular development, PLoS One 6 (2011) e22542.
[10] R.J. Deshaies, C.A. Joazeiro, RING domain E3 ubiquitin ligases, Annu. Rev. Biochem. 78 (2009) 399–434.
[11] S.R. White, B. Lauring, AAA + ATPases: achieving diversity of function with conserved machinery, Traffic 8 (2007) 1657–1667.
[12] M. Yoshioka, T. Kayo, T. Ikeda, A. Koizumi, A novel locus, Mody4, distal to D7Mit189 on chromosome 7 determines early-onset NIDDM in nonobese C57BL/6 (Akita) mutant mice, Diabetes 46 (1997) 887–894.
[13] J. Wang, T. Takeuchi, S. Tanaka, S.K. Kubo, T. Kayo, D. Lu, K. Takata, A. Koizumi, T. Izumi, A mutation in the insulin 2 gene induces diabetes with severe pancreatic beta-cell dysfunction in the Mody mouse, J. Clin. Invest. 103 (1999) 27–37.
[14] J. Nozaki, H. Kubota, H. Yoshida, M. Naitoh, J. Goji, T. Yoshinaga, K. Mori, A. Koizumi, K. Nagata, The endoplasmic reticulum stress response is stimulated through the continuous activation of transcription factors ATF6 and XBP1 in Ins2^{+}/Akita pancreatic beta cells, Genes Cells 9 (2004) 261–270.
[15] J. Miyazaki, K. Araki, E. Yamato, H. Ikegami, T. Asano, Y. Shibasaki, Y. Oka, K. Yamamura, Establishment of a pancreatic beta cell line that retains glucose-inducible insulin secretion: special reference to expression of glucose transporter isoforms, Endocrinology 127 (1990) 126–132.
[16] M. Toyoshima, A. Asakawa, M. Fujimiya, K. Inoue, S. Inoue, M. Kinboshi, A. Koizumi, Dimorphic gene expression patterns of anorexigenic and orexigenic peptides in hypothalamus account male and female hyperphagia in Akita type 1 diabetic mice, Biochem. Biophys. Res. Commun. 352 (2007) 703–708.
[17] M.S. Martin-Gronert, S.E. Ozanne, Metabolic programming of insulin action and secretion, Diabetes Obes. Metab. 14 (Suppl. 3) (2012) 29–39.
[18] S.J. Marciniak, C.Y. Yun, S. Oyadomari, I. Novoa, Y. Zhang, R. Jungreis, K. Nagata, H.P. Harding, D. Ron, CHOP induces death by promoting protein synthesis and oxidation in the stressed endoplasmic reticulum, Genes Dev. 18 (2004) 3066–3077.
[19] S. Yamane, Y. Hamamoto, S. Harashima, N. Harada, A. Hamasaki, K. Toyoda, K. Fujita, E. Joo, Y. Seino, N. Inagaki, GLP-1 receptor agonist attenuates endoplasmic reticulum stress-mediated β-cell damage in Akita mice, J. Diabetes Invest. 2 (2011) 104–110.
[20] A. Jurczyk, S.C. Pino, B. O'Sullivan-Murphy, M. Addorio, E.A. Lidstone, P. Diiorio, K.L. Lipson, C. Standley, K. Fogarty, L. Lifshitz, F. Urano, J.P. Mordes, D.L. Greiner, A.A. Rossini, R. Bortell, A novel role for the centrosomal protein, pericentrin, in regulation of insulin secretory vesicle docking in mouse pancreatic beta-cells, PLoS One 5 (2010) e11812.
[21] J.R. Allen, L.X. Nguyen, K.E. Sargent, K.L. Lipson, A. Hackett, F. Urano, High ER stress in beta-cells stimulates intracellular degradation of misfolded insulin, Biochem. Biophys. Res. Commun. 324 (2004) 166–170.
[22] M. Liu, I. Hodish, C.J. Rhodes, P. Arvan, Proinsulin maturation, misfolding, and proteotoxicity, Proc. Natl. Acad. Sci. USA 104 (2007) 15841–15846.